Journal of Mathematical Extension
Vol. 18, No. 11, (2024) (3) 1-35
ISSN: 1735-8299
URL: http://10.30495/JME.2024.3221
Original Research Paper

Stability and Numerical Simulation of an SCIRS Epidemic Model for Covid-19 Transmission by Caputo Derivative of Fractional Order

F. Janatolmakan
Azarbaijan Shahid Madani University

V. Roomi*
Azarbaijan Shahid Madani University

T. K. Gharahasanlou
Imam Hossein University

Abstract. In this paper, applying Caputo fractional derivative operator, the SCIRS epidemic model of Covid-19 has been presented. First, the well-definedness of the model (positive invariance) has been checked. We then calculate the equilibrium points of the system and the reproduction number and discuss the local and global stability of the equilibria based on values of the reproduction number. For the global stability of the rest points, the Liapunov's second method and LaSalle's invariance principle are used. The Pontryagin minimization principle is utilized to derive the optimal control conditions, with a focus on minimizing both the infection rate and the cost associated with vaccination implementation. Applying fixed point theory, the existence and uniqueness of the solutions of the model has been proven. Additionally, by using MATLAB and fractional Euler method, a numerical method has been applied to simulate the solutions based on real data and predict the transmission of Covid-19.

Received: December 2024; Accepted: February 2025
*Corresponding Author

AMS Subject Classification: 35A07; 35Q53
Keywords and Phrases: Basic reproduction number, Covid-19, Epidemiological modeling, Equilibrium point, Numerical simulation, SCIRS model

1 Introduction

In late 2019, a novel virus known as coronavirus rapidly spread worldwide at an unprecedented rate [29]. Its origins were traced back to the food market in Wuhan, China. Officially named SARS-CoV-2, this virus has caused over 500 million hospitalizations and claimed the lives of more than 6 million individuals globally [19]. Symptoms associated with this virus include cough, shortness of breath, weakness, lethargy, fever, chills, fatigue, muscle aches, sore throat, and more [3]. It can infect both humans and animals, with transmission occurring through inhalation of viral particles [1]. The disease is particularly severe in the elderly and individuals with underlying conditions such as cancer, cardiovascular disease, kidney and lung disorders, immune deficiency, and diabetes [24, 34, 48, 49]. Currently, there is no definitive cure for the virus, but various vaccines are being utilized to mitigate mortality and serious illness in infected and non-infected individuals [8, 41]. Complications resulting from this disease encompass acute respiratory distress syndrome (ARDS), blood clots, cardiac arrhythmias, cardiogenic shock, kidney damage or failure, heart damage, and ultimately, fatality [2, 13, 15, 17, 23, 31]. The most effective measures to prevent contracting this dangerous virus include the use of personal protective equipment like masks and gloves, regular handwashing, avoiding crowded environments, and receiving recommended vaccinations [22, 27, 38]. Evidence suggests that previous infection does not guarantee immunity against subsequent infections [12, 32, 45].

The use of differential equations with integer-order for epidemiological modeling of infectious diseases to investigate the dynamics of epidemic transmission is extensively studied [11, 14]. Thematic modeling of epidemic diseases demonstrates that nonlinear dynamic equations can offer valuable insights into the dynamics of disease transmission and dynamic diffusion behaviors. The global impact of Covid-19 (C-19) has garnered the attention of researchers interested in mathematical

modeling of this infectious disease. They have developed real nonlinear mathematical models driven by data to enhance our understanding of epidemic transmission dynamics (see, for instance, [36, 43].

Recently, differential equations with non-integer order or fractional order have been studied for modeling in applied mathematics. For example, the authors in [28] have studied an SEIARS model for analyzing C-19 pandemic process via ψ-Caputo fractional derivative. Also, in the study of illness such as C-19 [7, 46] and rabies [6], the authors have been applied fractional differential equations (FDEs) for modeling the spread of infection in human population. Also, authors have considered FDEs to study the another variants of problems, such as system of hybrid fractional differential equations [5] and fractional integro-differential equations [18, 40, 42].

FDEs serve as effective mathematical models for examining biological systems. These equations incorporate differential operators that capture the memory dynamics observed in many biological systems [9, 10]. Scientists have successfully applied the Caputo fractional order (CFO) to analyze the dynamics of various infectious diseases, such as HIV [30, 44] and Malaria [4, 33, 35]. Furthermore, in a study conducted by the authors of [39], they introduced an SEIR epidemic model that incorporated these equations to investigate the transmission of C-19.

The organization of the article is as follows: initially, it presents the necessary definitions for the study and introduces a fractional SCIRS model for the transmission of C-19. The EPs and reproduction numbers of the model will be calculated. Subsequently, the article analyzes the stability of the EPs and demonstrates the existence and uniqueness of the solution for the system. The optimal control of the system is analyzed by considering the intervention as a control strategy aimed at reducing the number of infected individuals. In the numerical section, the mathematical analysis and simulation of C-19 transmission is presented. To show the advantages of utilizing fractional derivatives, the article compares the results of the fractional and integer derivative models using real data. The aim is to determine which model offers a more integer approximation in this context. Additionally, the article examines how the derivative order affects the results and EPs by presenting findings for different orders of the fractional derivative.

Here, we begin by introducing the essential definitions of fractional calculus that are relevant to the present study.

Definition 1.1. *[21] For a function y, the Caputo fractional derivative (CFD) of order $\alpha \in (0,1)$ is given by*

$$^{C}\mathfrak{D}^{\alpha}y(t) = \frac{1}{\Gamma(n-\alpha)}\int_0^t \frac{y^{(n)}(x)dx}{(t-x)^{(\alpha-n+1)}}, \qquad n = [\alpha]+1.$$

Also, fractional integral of order α with $\alpha \in \mathbb{R}^+$ is defined as

$$^{C}\mathfrak{I}^{\alpha}y(t) = \frac{1}{\Gamma(\alpha)}\int_0^t (t-x)^{\alpha-1}y(x)dx.$$

Definition 1.2. *[21] The Laplace transform $\mathfrak{L}$ of the CFD of order α can be expressed as follows:*

$$\mathfrak{L}[^{C}\mathfrak{D}^{\alpha}y(t)](s) = s^{\alpha}\mathfrak{L}y(t) - \sum_{i=0}^{n-1} s^{\alpha-i-1}y^{(i)}(0), \quad n-1 < \alpha \leq n \in N.$$

Definition 1.3. *[21] The Mittag-Leffler function $\mathfrak{E}_{\alpha}(z)$ is defined by*

$$\mathfrak{E}_{\alpha}(z) := \sum_{k=0}^{\infty} \frac{z^k}{\Gamma(\alpha k+1)}, \quad (z \in \mathbb{C}; \Re(\alpha) > 0),$$

The generalized Mittag-Leffler function $\mathfrak{E}_{\alpha,\beta}$ is defined by

$$\mathfrak{E}_{\alpha,\beta}(z) := \sum_{k=0}^{\infty} \frac{z^k}{\Gamma(\alpha k+\beta)}, \quad (z, \beta \in \mathbb{C}; \Re(\alpha) > 0).$$

2 Model Framework

Mathematical models play a vital role in forecasting the spread of viruses during viral outbreaks by considering their patterns in various geographical areas. A range of mathematical models, including SIR, SEIAR, SIRS, SCIR, and SIQR are employed to explore the occurrence of diseases. As per the World Health Organization's information on C-19,

Table 1

Parameters	The biological interpretation
Λ	the recruitment rate
μ	the natural death rate
β	the transmission rate of infection
γ	the recovery rate of asymptomatic individuals
σ	the recovery rate of infected individuals
δ	the death rate caused by the disease
η	the per capita rate of becoming infectious
ρ	improved susceptibility rate

there exist individuals who are asymptomatic carriers and can transmit disease-causing microorganisms without exhibiting any symptoms of infection. Furthermore, there are individuals within this group who might undergo reinfection even after they have recovered. Hence, we take into account the following SCIRS fractional model for C-19 in which the susceptible, carrier, symptomatic, and recovered compartments are represented by $\mathcal{S}$, $\mathcal{C}$, $\mathcal{I}$, and $\mathcal{R}$, respectively.

$$\begin{cases} \vartheta^{\alpha-1C}\mathfrak{D}_t^{\alpha}\mathcal{S}(t) = \Lambda - \beta\mathcal{S}(\mathcal{I}+q\mathcal{C}) - \mu\mathcal{S} + \rho\mathcal{R}, \\ \vartheta^{\alpha-1C}\mathfrak{D}_t^{\alpha}\mathcal{C}(t) = \beta\mathcal{S}(\mathcal{I}+q\mathcal{C}) - (\eta+\gamma+\mu)\mathcal{C}, \\ \vartheta^{\alpha-1C}\mathfrak{D}_t^{\alpha}\mathcal{I}(t) = \eta\mathcal{C} - (\sigma+\mu+\delta)\mathcal{I}, \\ \vartheta^{\alpha-1C}\mathfrak{D}_t^{\alpha}\mathcal{R}(t) = \sigma\mathcal{I} + \gamma\mathcal{C} - (\mu+\rho)\mathcal{R}, \end{cases} \tag{1}$$

where $t > 0$ and $\alpha \in (0, 1)$.

The initial conditions are specified as follows: $\mathcal{S}(0) = \mathcal{S}_0 > 0$, $\mathcal{C}(0) = \mathcal{C}_0 > 0$, $\mathcal{I}(0) = \mathcal{I}_0 > 0$, $\mathcal{R}(0) = \mathcal{R}_0 \geq 0$. Also, the parameters are introduced in Table 1.

Nonnegative solution:
Let $\Omega = \{(\mathcal{S}, \mathcal{C}, \mathcal{I}, \mathcal{R}) \in \Re_4^+ : \mathcal{S}+\mathcal{C}+\mathcal{I}+\mathcal{R} \leq \frac{\Lambda}{\mu}\}$. We demonstrate that the closed set Ω represents the region of feasibility for system (1).

Lemma 2.1. *The fractional system (1) exhibits positive invariance with respect to the closed set* Ω.

Proof. Accordingly, by summing up all the equations in system (1), we can obtain the fractional derivative of the total population. Thus,

$$\vartheta^{\alpha-1}{}^{C}\mathfrak{D}_t^{\alpha}\mathcal{N}(t) = \Lambda - \mu\mathcal{N}(t) - \delta\mathcal{I}(t) \leq \Lambda - \mu\mathcal{N}(t),$$

where $\mathcal{N}(t) = \mathcal{S}(t) + \mathcal{C}(t) + \mathcal{I}(t) + \mathcal{R}(t)$. By employing the $\mathfrak{L}\{\mathcal{N}(t)\}$ and utilizing Theorem 7.2 in [16], we arrive at the result of

$$\mathcal{N}(t) \leq \mathcal{N}(0)\mathfrak{E}_{\alpha}(-\mu\vartheta^{1-\alpha}t^{\alpha}) + \int_0^t \Lambda\vartheta^{1-\alpha}\eta^{\alpha-1}\mathfrak{E}_{\alpha,\alpha}(-\mu\vartheta^{1-\alpha}\eta^{\alpha})d\eta,$$

where $\mathcal{N}(0)$ denotes the initial size of the population. Therefore, using the series expansion of Mittag-Leffler functions

$$\begin{aligned}\mathcal{N}(t) &\leq \mathcal{N}(0)\mathfrak{E}_{\alpha}(-\mu\vartheta^{1-\alpha}t^{\alpha}) + \int_0^t \Lambda\vartheta^{1-\alpha}\eta^{\alpha-1}\sum_{k=0}^{\infty}\frac{(-1)^k\mu^k\vartheta^{k(1-\alpha)}\eta^{k\alpha}}{\Gamma(k\alpha+\alpha)}d\eta \\ &= \frac{\Lambda\vartheta^{1-\alpha}}{\mu\vartheta^{1-\alpha}} + \mathfrak{E}_{\alpha}(-\mu\vartheta^{1-\alpha}t^{\alpha})(\mathcal{N}(0) - \frac{\Lambda\vartheta^{1-\alpha}}{\mu\vartheta^{1-\alpha}}) \\ &= \frac{\Lambda}{\mu} + \mathfrak{E}_{\alpha}(-\mu\vartheta^{1-\alpha}t^{\alpha})(\mathcal{N}(0) - \frac{\Lambda}{\mu}).\end{aligned}$$

Thus, if $\mathcal{N}(0) \leq \frac{\Lambda}{\mu}$, then $\mathcal{N}(t) \leq \frac{\Lambda}{\mu}$ for $t > 0$. As a result, the model ensures that the closed set Ω remains invariant in a positive manner. □

3 Equilibrium Points

The approach outlined in [47] is utilized to calculate the basic reproduction number ($\mathcal{R}_0$) of the model. To determine $\mathcal{R}_0$, we rewrite the second and third equations of (1) as:

$$^{C}\mathfrak{D}^{\alpha}\Psi = \mathfrak{F}(\Psi) - \mathfrak{V}(\Psi),$$

where

$$\Psi = \begin{bmatrix}\mathcal{C}\\ \mathcal{I}\end{bmatrix}, \quad \mathfrak{F}(\Psi) = \vartheta^{1-\alpha}\begin{bmatrix}\beta\mathcal{S}(\mathcal{I}+q\mathcal{C})\\ \eta\mathcal{C}\end{bmatrix}, \quad \mathfrak{V}(\Psi) = \vartheta^{1-\alpha}\begin{bmatrix}(\eta+\gamma+\mu)\mathcal{C}\\ (\sigma+\mu+\delta)\mathcal{I}\end{bmatrix}.$$

At $\mathcal{E}_0$, the Jacobian matrices for $\mathfrak{F}$ and $\mathfrak{V}$ are obtained as follows:

$$\mathfrak{J}_{\mathfrak{F}}(\mathcal{E}_0) = \vartheta^{1-\alpha}\begin{bmatrix} \beta\mathcal{S}q & \beta\mathcal{S} \\ \eta & 0 \end{bmatrix}, \quad \mathfrak{J}_{\mathfrak{V}}(\mathcal{E}_0) = \vartheta^{1-\alpha}\begin{bmatrix} (\eta+\gamma+\mu) & 0 \\ 0 & (\sigma+\mu+\delta) \end{bmatrix}.$$

The reproduction number $\mathcal{R}_0$ is calculated based on the spectral radius of matrix $\mathfrak{J}_{\mathfrak{F}}\mathfrak{J}_{\mathfrak{V}}^{-1}$ which is equal to

$$\mathcal{R}_0 = \frac{\beta\Lambda q}{\mu(\eta+\gamma+\mu)} + \frac{\beta\Lambda\eta}{\mu(\eta+\gamma+\mu)(\sigma+\mu+\delta)} = \mathcal{R}_{01} + \mathcal{R}_{02}. \tag{2}$$

It serves as an epidemiological measure to assess the degree of contagiousness or transmissibility exhibited by infectious agents.

To determine the EPs of system (1), we equate the equations of the fractional system to zero. By solving the resulting algebraic equations, we can determine the EPs of system (1). The EP corresponding to the absence of disease is attained as $\mathcal{E}_0 = (\frac{\Lambda}{\mu}, 0, 0, 0)$. Moreover, if $\mathcal{R}_0 > 1$, the system (1) exhibits a positive endemic EP $\mathcal{E}_1 = (\mathcal{S}^*, \mathcal{C}^*, \mathcal{I}^*, \mathcal{R}^*)$, where

$$\begin{aligned}
\mathcal{S}^* &= \frac{(\sigma+\mu+\delta)(\eta+\gamma+\mu)}{\beta\eta+\beta q(\sigma+\mu+\delta)}, \\
\mathcal{C}^* &= \frac{(\sigma+\mu+\delta)\mathcal{I}}{\eta}, \\
\mathcal{R}^* &= \frac{\sigma\mathcal{I}}{(\mu+\rho)} + \frac{\gamma(\sigma+\mu+\delta)\mathcal{I}}{(\mu+\rho)\eta}, \\
\mathcal{I}^* &= \frac{\mu(\eta+\gamma+\mu)(\sigma+\mu+\delta)(\mu+\rho)\eta}{AB}[\mathcal{R}_0 - 1],
\end{aligned}$$

where

$$\begin{aligned}
A &= [\eta\beta + \beta q(\sigma+\mu+\delta)], \\
B &= [(\eta+\gamma+\mu)(\sigma+\mu+\delta)(\mu+\rho) + \rho\sigma\eta + \rho\gamma(\sigma+\mu+\delta)].
\end{aligned}$$

4 $\mathcal{R}_0$ Sensitivity Analysis

In this analysis, we will explore the sensitivity of $\mathcal{R}_0$. Analyzing the sensitivity of the endemic threshold $\mathcal{R}_0$ provides valuable insights into

the importance of individual parameters in the transmission of a disease. This knowledge is essential not only for designing experiments, but also for incorporating data and simplifying intricate models [37]. Sensitivity analysis is frequently employed to evaluate the resilience of model predictions when parameter values vary, considering data collection errors and assumed parameter values. It aids in identifying parameters that exert a substantial influence on the threshold $\mathcal{R}_0$ and should be focused on intervention strategies. To be more specific, sensitivity indices allow us to measure the proportional change in a variable when a parameter is altered. To assess the sensitivity of $\mathcal{R}_0$, we compute its derivatives as follows:

$$\begin{aligned}
\frac{\partial \mathcal{R}_0}{\partial \beta} &= \frac{\mathcal{S}^* q}{(\eta+\gamma+\mu)} + \frac{\eta \mathcal{S}^*}{(\eta+\gamma+\mu)(\sigma+\mu+\delta)},\\
\frac{\partial \mathcal{R}_0}{\partial \eta} &= \frac{-\beta \mathcal{S}^* q}{(\eta+\gamma+\mu)^2} + \frac{\beta \mathcal{S}^*}{(\eta+\gamma+\mu)(\sigma+\mu+\delta)} - \frac{\eta\beta \mathcal{S}^*}{(\eta+\gamma+\mu)^2(\sigma+\mu+\delta)},\\
\frac{\partial \mathcal{R}_0}{\partial \gamma} &= \frac{-\beta \mathcal{S}^* q}{(\eta+\gamma+\mu)^2} - \frac{\eta\beta \mathcal{S}^*}{(\eta+\gamma+\mu)^2(\sigma+\mu+\delta)},\\
\frac{\partial \mathcal{R}_0}{\partial \delta} &= \frac{-\eta\beta \mathcal{S}^*}{(\eta+\gamma+\mu)(\sigma+\mu+\delta)^2},\\
\frac{\partial \mathcal{R}_0}{\partial \alpha} &= \frac{-\eta\beta \mathcal{S}^*}{(\eta+\gamma+\mu)(\sigma+\mu+\delta)^2},\\
\frac{\partial \mathcal{R}_0}{\partial \mu} &= \frac{-\beta \mathcal{S}^* q}{(\eta+\gamma+\mu)^2} - \frac{\eta\beta \mathcal{S}^*}{(\eta+\gamma+\mu)^2(\sigma+\mu+\delta)} - \frac{\eta\beta \mathcal{S}^*}{(\eta+\gamma+\mu)(\sigma+\mu+\delta)^2}.
\end{aligned}$$

Since all the parameters are positive, $\frac{\partial \mathcal{R}_0}{\partial \beta} > 0$. Thus, $\mathcal{R}_0$ is rising in conjunction with β, and is decreasing with γ, δ, σ and μ. But we cannot say anything about η here.

5 Stability of Equilibria

The primary aim of this section is to assess the stability of the EPs. We first compute the Jacobian matrix ($\mathfrak{J}$) for system (1) as follows:

$$\mathfrak{J} = \vartheta^{1-\alpha} \begin{bmatrix} -\beta(\mathcal{I}+q\mathcal{C}) - \mu & -\beta \mathcal{S} q & -\beta \mathcal{S} & \rho \\ \beta(\mathcal{I}+q\mathcal{C}) & \beta \mathcal{S} q - (\eta+\gamma+\mu) & \beta \mathcal{S} & 0 \\ 0 & \eta & -(\sigma+\mu+\delta) & 0 \\ 0 & \gamma & \sigma & -(\mu+\rho) \end{bmatrix}.$$

As a result,

$$\mathfrak{J}(\mathcal{E}_0) = \vartheta^{1-\alpha}\begin{bmatrix} -\mu & -\beta\mathcal{S}^0 q & -\beta\mathcal{S}^0 & \rho \\ 0 & \beta\mathcal{S}^0 q - (\eta+\gamma+\mu) & \beta\mathcal{S}^0 & 0 \\ 0 & \eta & -(\sigma+\mu+\delta) & 0 \\ 0 & \gamma & \sigma & -(\mu+\rho) \end{bmatrix},$$

where $\mathcal{S}^0 = \dfrac{\Lambda}{\mu}$.

Theorem 5.1. *If $\mathcal{R}_0$ is less than 1, then the EP $\mathcal{E}_0$ is locally asymptotically stable (LAS). Conversely, if $\mathcal{R}_0$ is greater than 1, then $\mathcal{E}_0$ is unstable.*

Proof. Let us analyze the equation $|\mathfrak{J} - \lambda I| = 0$. It is easy to see that $\lambda_1 = -\mu$ is an eigenvalue. Afterward, by expanding the remaining matrix around the last column, we acquire an eigenvalue as $\lambda_2 = -(\mu + \rho)$. The remaining pair of eigenvalues are associated with the eigenvalues of the subsequent matrix:

$$\mathfrak{J}_1 = \vartheta^{1-\alpha}\begin{bmatrix} \beta\mathcal{S}^0 q - (\eta+\gamma+\mu) & \beta\mathcal{S}^0 \\ \eta & -(\sigma+\mu+\delta) \end{bmatrix}.$$

Next, we can utilize the standard criteria that guarantee the eigenvalue of J_1 possess a negative real component. Specifically, we need to fulfill the conditions $Tr(\mathfrak{J}_1) < 0$ and $Det(\mathfrak{J}_1) > 0$. The second inequality leads to the condition $-[\beta\mathcal{S}^0 q - (\eta+\gamma+\mu)](\sigma+\mu+\delta) - \eta\beta\mathcal{S}^0 > 0$ which establishes $\mathcal{R}_0$ in the form of (2).

It is important to highlight that when $\mathcal{R}_0 < 1$, both inequalities $Tr(\mathfrak{J}_1) < 0$ and $Det(\mathfrak{J}_1) > 0$ are also fulfilled. Consequently, if $\mathcal{R}_0 < 1$, the disease-free EP exhibits stability in the local asymptotic sense. On the other hand, if $\mathcal{R}_0 > 1$, the disease-free EP is unstable. □

The Jacobian matrix at the endemic EP is as:

$$\mathfrak{J}(\mathcal{E}_1) = \vartheta^{1-\alpha}\begin{bmatrix} -\beta(\mathcal{I}^* + q\mathcal{C}^*) - \mu & -\beta\mathcal{S}^* q & -\beta\mathcal{S}^* & \rho \\ \beta(\mathcal{I}^* + q\mathcal{C}^*) & \beta\mathcal{S}^* q - (\eta+\gamma+\mu) & \beta\mathcal{S}^* & 0 \\ 0 & \eta & -(\sigma+\mu+\delta) & 0 \\ 0 & \gamma & \sigma & -(\mu+\rho) \end{bmatrix}.$$

Now, let us consider $|\mathfrak{J} - \lambda I| = 0$. Through the expansion of the determinant, we obtain the characteristic equation of the endemic EP in the following manner:

$$\lambda^3 + A_1\lambda^2 + A_2\lambda + A_3 = 0,$$

where

$$\begin{aligned}
A_1 &= \frac{1}{\mu}(\sigma + 3\mu + \delta + \rho + \eta + \gamma),\\
A_2 &= \frac{1}{\mu}(\eta + \gamma + \mu)(\sigma + \mu + \delta) - \frac{1}{\beta\mu(\mathcal{I}^* + q\mathcal{C}^*)}[\beta\mathcal{S}^*\eta\mu + \rho\gamma],\\
A_3 &= \frac{1}{\beta\mu(\mathcal{I}^* + q\mathcal{C}^*)}[(\eta + \gamma + \mu)(\sigma + \mu + \delta)(\mu + \rho)\\
&\quad + (\eta + \gamma + \mu^2 + \sigma + \delta - \beta\mathcal{S}^*\eta\mu)(\mu + \rho) - \rho\gamma(\sigma + \mu + \delta)] - \rho\sigma\eta.
\end{aligned}$$

According to the Routh-Hurwitz stability criterion, the endemic equilibrium point $\mathcal{E}_1$ is locally asymptotically stable if and only if conditions $A_1 > 0, A_2 > 0, A_3 > 0$ and $A_1A_2 > A_3$ are satisfied. The positivity of the system parameters ensures that the coefficient A_1 is consistently positive. Therefore, EP $\mathcal{E}_1$ is LAS if $A_2 > 0, A_3 > 0$ and $A_1A_2 > A_3$.

Theorem 5.2. *The EP $\mathcal{E}_0$ of system is globally asymptotically stable (GAS) if $\mathcal{R}_{01} < \frac{1}{2}$ and $\mathcal{R}_{02} < \frac{1}{2}$.*

Proof. Consider the Lyapunov function:

$$\mathcal{V}_0(\mathcal{S}, \mathcal{C}, \mathcal{I}, \mathcal{R}) = \mathcal{S} - \mathcal{S}^0 - \mathcal{S}^0 \ln(\frac{\mathcal{S}}{\mathcal{S}^0}) + \mathcal{C} + \mathfrak{A}_1\mathcal{I} + \mathfrak{A}_2\mathcal{R},$$

where

$$\begin{aligned}
\mathfrak{A}_1 &= \frac{2\beta\mathcal{S}^0 + (\sigma + \mu + \delta)(\eta + \gamma + \mu)}{\eta(\eta + \sigma + \mu + \delta)},\\
\mathfrak{A}_2 &= \frac{(\sigma + \mu + \delta)(\eta + \gamma + \mu)[1 - 2\mathcal{R}_{02}]}{2\gamma(\eta + \sigma + \mu + \delta)}.
\end{aligned}$$

Computing the time derivative of $\mathcal{V}_0$ along the solution of (1) and using

equilibrium conditions, we have:

$$\begin{aligned}
\dot{\mathcal{V}}_0 &= (1-\frac{\mathcal{S}^0}{\mathcal{S}})\dot{\mathcal{S}}+\dot{\mathcal{C}}+\mathfrak{A}_1\dot{\mathcal{I}}+\mathfrak{A}_2\dot{\mathcal{R}}\\
&= (1-\frac{\mathcal{S}^0}{\mathcal{S}})[\Lambda-\beta\mathcal{S}(\mathcal{I}+q\mathcal{C})-\mu\mathcal{S}+\rho\mathcal{R}]+\beta\mathcal{S}(\mathcal{I}+q\mathcal{C})\\
&\quad -(\eta+\gamma+\mu)\mathcal{C}+\mathfrak{A}_1[\eta\mathcal{C}-(\sigma+\mu+\delta)\mathcal{I}]+\mathfrak{A}_2[\sigma\mathcal{I}+\gamma\mathcal{C}-(\mu+\rho)\mathcal{R}]\\
&= \Lambda(2-\frac{\mathcal{S}^0}{\mathcal{S}}-\frac{\mathcal{S}}{\mathcal{S}^0})+\rho(\frac{\mathcal{S}-\mathcal{S}^0}{\mathcal{S}})+\mathcal{I}[\frac{\beta\eta\mathcal{S}^0}{(\sigma+\mu+\delta)(\eta+\gamma+\mu)}-\frac{1}{2}]\\
&\quad +\mathcal{C}[\frac{2\beta q\mathcal{S}^0}{\eta+\gamma+\mu}-1]\\
&= \Lambda(2-\frac{\mathcal{S}^0}{\mathcal{S}}-\frac{\mathcal{S}}{\mathcal{S}^0})+\rho(\frac{\mathcal{S}-\mathcal{S}^0}{\mathcal{S}})+\mathcal{I}[\mathcal{R}_{01}-\frac{1}{2}]+\mathcal{C}[2\mathcal{R}_{02}-1]
\end{aligned}$$

Therefore, $\mathcal{S}-\mathcal{S}^0\leq 0$ and $2-\frac{\mathcal{S}^0}{\mathcal{S}}-\frac{\mathcal{S}}{\mathcal{S}^0}\leq 0$. Since $\mathcal{R}_{01}<\frac{1}{2}$ and $\mathcal{R}_{02}<\frac{1}{2}$, it can be concluded that $\dot{\mathcal{V}}_0\leq 0$ for all $\mathcal{S},\mathcal{C},\mathcal{I},\mathcal{R}>0$. Hence, the disease-free equilibrium $\mathcal{E}_0$ is stable. On the other hand, $\dot{\mathcal{V}}_0=0$ if and only if $\mathcal{S}=\mathcal{S}^0$, $\mathcal{C}=0$, $\mathcal{I}=0$ and $\mathcal{R}=0$. Let Ω_0 be the largest invariant set in

$$\Psi_0=\{(\mathcal{S},\mathcal{C},\mathcal{I},\mathcal{R})|\dot{\mathcal{V}}_0=0\}.$$

We have that $\Omega_0=\{\mathcal{E}_0\}$. The GAS of $\mathcal{E}_0$ follows from LaSalle's invariance principle. □

6 Optimal Control Approach

In this section, we examine the impact of vaccination on the recovery of C-19 patients using an optimal control strategy applied to the fractional SCIRS model (1). The control variable $u(t)$, representing the vaccination, is analyzed. Based on the provided explanations, we propose the following fractional control system

$$\begin{aligned}
{}^{\vartheta^{\alpha-1}C}\mathfrak{D}_t^{\alpha}\mathcal{S}(t) &= \Lambda-\beta\mathcal{S}(\mathcal{I}+q\mathcal{C})-(\mu+u(t))\mathcal{S}+\rho\mathcal{R},\\
{}^{\vartheta^{\alpha-1}C}\mathfrak{D}_t^{\alpha}\mathcal{C}(t) &= \beta\mathcal{S}(\mathcal{I}+q\mathcal{C})-(\eta+\gamma+\mu)\mathcal{C},\\
{}^{\vartheta^{\alpha-1}C}\mathfrak{D}_t^{\alpha}\mathcal{I}(t) &= \eta\mathcal{C}-(\sigma+\mu+\delta)\mathcal{I}(t),\\
{}^{\vartheta^{\alpha-1}C}\mathfrak{D}_t^{\alpha}\mathcal{R}(t) &= \sigma\mathcal{I}+\gamma\mathcal{C}+u(t)S-(\mu+\rho)\mathcal{R}. \qquad (3)
\end{aligned}$$

The fractional control system simplifies to system (1) when the control u is set to zero. The Pontryagin minimization principle ([20]) serves as the foundation for optimal control theory in fractional-order systems. The control $u(t)$ represent the fraction of vaccinated individuals per unit time at t. The cost function to be considered under the dynamic constraints (3) is as follows:

$$\mathfrak{L}(u) = \int_0^T [a_1\mathcal{C}(t) + a_2\mathcal{I}(t) + \frac{1}{2}a_3u^2(t)]dt \tag{4}$$

In (4), T is the duration of vaccination and the parameters a_1 and a_2 represent the weighting coefficient for the number of infected individuals $\mathcal{C}$ and $\mathcal{I}$. Also, a_3 denotes the cost associated with implementing the control strategy. By finding the optimal control u^* where $\mathfrak{L}(u^*) = \min \mathfrak{L}(u)$, we minimize the cost function $\mathfrak{L}(u)$.

Theorem 6.1. *Let $u(t) \in [0,1]$ to be a measurable function in $[0,T]$. Then, optimal control*

$$u^* = \max\{\min\{\frac{(\lambda_1 - \lambda_4)\vartheta^{1-\alpha}\mathcal{S}(t)}{a_3}, 1\}, 0\}$$

minimizes the function $\mathfrak{L}(u)$ subject to system (3).

Proof. To apply the Pontryagain minimization approach, we define the Hamiltonian as follows:

$$\begin{aligned}
\mathfrak{H} &= [a_1\mathcal{C}(t) + a_2\mathcal{I}(t) + \frac{1}{2}a_3u^2(t)] \\
&+ \lambda_1\vartheta^{1-\alpha}[\Lambda - \beta\mathcal{S}(\mathcal{I} + q\mathcal{C}) - (\mu + u(t))\mathcal{S} + \rho\mathcal{R}] \\
&+ \lambda_2\vartheta^{1-\alpha}[\beta\mathcal{S}(\mathcal{I} + q\mathcal{C}) - (\eta + \gamma + \mu)\mathcal{C}] \\
&+ \lambda_3\vartheta^{1-\alpha}[\eta\mathcal{C} - (\sigma + \mu + \delta)\mathcal{I}(t)] \\
&+ \lambda_4\vartheta^{1-\alpha}[\sigma\mathcal{I} + \gamma\mathcal{C} + u(t)S - (\mu + \rho)\mathcal{R}]
\end{aligned}$$

where the adjoint variables are $\lambda_i(t), i = 1, ..., 4$ with $\lambda_i(T) = 0$. Also,

they satisfy in the following system

$$\begin{aligned}
\vartheta^{\alpha-1C}\mathfrak{D}_t^{\alpha}\lambda_1(t) &= -\frac{\partial \mathfrak{H}}{\partial \mathcal{S}} = \lambda_1[\beta(\mathcal{I}-(\mu+u(t))] - \lambda_2[\beta(\mathcal{I}+q\mathcal{C})] - \lambda_4 u,\\
\vartheta^{\alpha-1C}\mathfrak{D}_t^{\alpha}\lambda_2(t) &= -\frac{\partial \mathfrak{H}}{\partial \mathcal{C}} = \lambda_1(\beta\mathcal{S}q) - \lambda_2[\beta\mathcal{S}q-(\eta+\gamma+\mu)] - \lambda_3\eta - \lambda_4\gamma - a_1,\\
\vartheta^{\alpha-1C}\mathfrak{D}_t^{\alpha}\lambda_3(t) &= -\frac{\partial \mathfrak{H}}{\partial \mathcal{I}} = \lambda_1\beta\mathcal{S} - \lambda_2\beta\mathcal{S} + \lambda_3(\sigma+\mu+\delta) - \lambda_4\sigma - a_2,\\
\vartheta^{\alpha-1C}\mathfrak{D}_t^{\alpha}\lambda_4(t) &= -\frac{\partial \mathfrak{H}}{\partial \mathcal{R}} = -\lambda_1\rho + \lambda_4(\mu+\rho). \qquad (5)
\end{aligned}$$

To determine $u(t)$, we minimize the Hamiltonian function by adjusting the control variable. By applying the Pontryagin principle, we obtain the following optimality condition:

$$\frac{\partial \mathfrak{H}}{\partial u} = 0 \Longrightarrow u = \frac{(\lambda_1-\lambda_4)\vartheta^{1-\alpha}\mathcal{S}(t)}{a_3}.$$

Consequently, $u(t)$, the ideal control variable, is obtained as

$$u^* = \max\{\min\{\frac{(\lambda_1-\lambda_4)\vartheta^{1-\alpha}\mathcal{S}(t)}{a_3}, 1\}, 0\}.$$

By solving the problems (3) and (5), the optimal control is calculated. □

7 Existence and Uniqueness of Solutions

In this section, applying the fixed point theorem, the existence and uniqueness of solutions for system (1) will be shown. The method of Nieto and Losada ([26]) will be applied on equation (1). To initiate this process, we reformulate the system mentioned in equation (1) in the subsequent form:

$$\begin{cases}
\vartheta^{\alpha-1C}\mathfrak{D}_t^{\alpha}\mathcal{S}(t) = \mathfrak{L}_1(t,\mathcal{S}(t)),\\
\vartheta^{\alpha-1C}\mathfrak{D}_t^{\alpha}\mathcal{C}(t) = \mathfrak{L}_2(t,\mathcal{C}(t)),\\
\vartheta^{\alpha-1C}\mathfrak{D}_t^{\alpha}\mathcal{I}(t) = \mathfrak{L}_3(t,\mathcal{I}(t)),\\
\vartheta^{\alpha-1C}\mathfrak{D}_t^{\alpha}\mathcal{R}(t) = \mathfrak{L}_4(t,\mathcal{R}(t)).
\end{cases}$$

By integrating both sides, we obtain

$$\begin{cases} \mathcal{S}(t) - \mathcal{S}(0) = \dfrac{\vartheta^{1-\alpha}}{\Gamma(\alpha)} \displaystyle\int_0^t \mathfrak{L}_1(\tau, \mathcal{S})(t-\tau)^{\alpha-1} d\tau, \\ \mathcal{C}(t) - \mathcal{C}(0) = \dfrac{\vartheta^{1-\alpha}}{\Gamma(\alpha)} \displaystyle\int_0^t \mathfrak{L}_2(\tau, \mathcal{C})(t-\tau)^{\alpha-1} d\tau, \\ \mathcal{I}(t) - \mathcal{I}(0) = \dfrac{\vartheta^{1-\alpha}}{\Gamma(\alpha)} \displaystyle\int_0^t \mathfrak{L}_3(\tau, \mathcal{I})(t-\tau)^{\alpha-1} d\tau, \\ \mathcal{R}(t) - \mathcal{R}(0) = \dfrac{\vartheta^{1-\alpha}}{\Gamma(\alpha)} \displaystyle\int_0^t \mathfrak{L}_4(\tau, \mathcal{R})(t-\tau)^{\alpha-1} d\tau. \end{cases} \tag{6}$$

We prove that the kernels $\mathfrak{L}_i$, with $i = 1, 2, 3, 4$, satisfy the Lipschitz condition (LC) and contraction properties.

Theorem 7.1. *Let $f_1 = \beta d_3 + q\beta d_2 + \mu$ in which d_2 and d_3 are upper bounds for $\mathcal{C}(t)$ and $\mathcal{I}(t)$, respectively. Then, $\mathfrak{L}_1$ satisfies LC and if $0 \leq f_1 < 1$, then it is also a contraction.*

Proof. For $\mathcal{S}$ and $\mathcal{S}_1$ we have

$$\begin{aligned} ||\mathfrak{L}_1(t, \mathcal{S}) - \mathfrak{L}_1(t, \mathcal{S}_1)|| &= || - \beta(\mathcal{S}(t) - \mathcal{S}_1(t))(\mathcal{I} + q\mathcal{C}) - \mu(\mathcal{S}(t) - \mathcal{S}_1(t)) + \rho\mathcal{R}|| \\ &\leq ||\beta\mathcal{I}(t) + q\beta\mathcal{C}(t)||||\mathcal{S}(t) - \mathcal{S}_1(t)|| + \mu||\mathcal{S}(t) - \mathcal{S}_1(t)|| \\ &\leq (\beta||\mathcal{I}(t)|| + q\beta||\mathcal{C}(t)|| + \mu)||\mathcal{S}(t) - \mathcal{S}_1(t)|| \\ &\leq (\beta d_3 + q\beta d_2 + \mu)||\mathcal{S}(t) - \mathcal{S}_1(t)||. \end{aligned}$$

Therefore,

$$||\mathfrak{L}_1(t, \mathcal{S}) - \mathfrak{L}_1(t, \mathcal{S}_1)|| \leq f_1||(\mathcal{S}(t) - \mathcal{S}_1(t))||. \tag{7}$$

Thus, LC for $\mathfrak{L}_1$ is achieved, and if $0 \leq \beta d_3 + q\beta d_2 + \mu < 1$, then $\mathfrak{L}_1$ is a contraction. □

Similarly, we can demonstrate that $\mathfrak{L}_j$, where $j = 2, 3, 4$, satisfies LC as:

$$\begin{aligned} ||\mathfrak{L}_2(t, \mathcal{C}) - \mathfrak{L}_2(t, \mathcal{C}_1)|| &\leq f_2||(\mathcal{C}(t) - \mathcal{C}_1(t))||, \\ ||\mathfrak{L}_3(t, \mathcal{I}) - \mathfrak{L}_3(t, \mathcal{I}_1)|| &\leq f_3||(\mathcal{I}(t) - \mathcal{I}_1(t))||, \\ ||\mathfrak{L}_4(t, \mathcal{R}) - \mathfrak{L}_4(t, \mathcal{R}_1)|| &\leq f_4||(\mathcal{R}(t) - \mathcal{R}_1(t))||, \end{aligned}$$

in which $||\mathcal{S}(t)|| \leq d_1$, and $f_2 = \beta q d_1 + (\eta + \gamma + \mu)$, $f_3 = \sigma + \mu + \delta$ and $f_4 = \mu + \rho$. If $0 \leq f_j < 1$ for $j = 2, 3, 4$, then $\mathfrak{L}_j$ are also contraction mappings.

Considering system (6) as a basis, we can express the following recursive forms:

$$\phi_{1,n}(t) = \mathcal{S}_n(t) - \mathcal{S}_{n-1}(t) = \frac{\vartheta^{1-\alpha}}{\Gamma(\alpha)} \int_0^t (\mathfrak{L}_1(\tau, \mathcal{S}_{n-1}) - \mathfrak{L}_1(\tau, \mathcal{S}_{n-2}))(t-\tau)^{\alpha-1} d\tau,$$
$$\phi_{2,n}(t) = \mathcal{C}_n(t) - \mathcal{C}_{n-1}(t) = \frac{\vartheta^{1-\alpha}}{\Gamma(\alpha)} \int_0^t (\mathfrak{L}_2(\tau, \mathcal{C}_{n-1}) - \mathfrak{L}_2(\tau, \mathcal{C}_{n-2}))(t-\tau)^{\alpha-1} d\tau,$$
$$\phi_{3,n}(t) = \mathcal{I}_n(t) - \mathcal{I}_{n-1}(t) = \frac{\vartheta^{1-\alpha}}{\Gamma(\alpha)} \int_0^t (\mathfrak{L}_3(\tau, \mathcal{I}_{n-1}) - \mathfrak{L}_3(\tau, \mathcal{I}_{n-2}))(t-\tau)^{\alpha-1} d\tau,$$
$$\phi_{4,n}(t) = \mathcal{R}_n(t) - \mathcal{R}_{n-1}(t) = \frac{\vartheta^{1-\alpha}}{\Gamma(\alpha)} \int_0^t (\mathfrak{L}_4(\tau, \mathcal{R}_{n-1}) - \mathfrak{L}_4(\tau, \mathcal{R}_{n-2}))(t-\tau)^{\alpha-1} d\tau,$$

with the initial conditions$(\mathcal{S}(0), \mathcal{C}(0), \mathcal{I}(0), \mathcal{R}(0)) = (\mathcal{S}_0, \mathcal{C}_0, \mathcal{I}_\prime, \mathcal{R}_0)$. We have

$$\begin{aligned} ||\phi_{1,n}(t)|| &= ||\mathcal{S}_n(t) - \mathcal{S}_{n-1}(t)|| \\ &= ||\frac{\vartheta^{1-\alpha}}{\Gamma(\alpha)} \int_0^t (\mathfrak{L}_1(\tau, \mathcal{S}_{n-1}) - \mathfrak{L}_1(\tau, \mathcal{S}_{n-2}))(t-\tau)^{\alpha-1} d\tau|| \\ &\leq \frac{\vartheta^{1-\alpha}}{\Gamma(\alpha)} \int_0^t ||(\mathfrak{L}_1(\tau, \mathcal{S}_{n-1}) - \mathfrak{L}_1(\tau, \mathcal{S}_{n-2}))(t-\tau)^{\alpha-1}|| d\tau. \end{aligned}$$

Impose LC (7) to get

$$||\phi_{1,n}(t)|| \leq \frac{\vartheta^{1-\alpha}}{\Gamma(\alpha)} f_1 \int_0^t ||\phi_{1,n-1}(\tau)|| d\tau. \tag{8}$$

Similarly, we obtain

$$\begin{aligned} ||\phi_{2,n}(t)|| &\leq \frac{\vartheta^{1-\alpha}}{\Gamma(\alpha)} f_2 \int_0^t ||\phi_{2,n-1}(\tau)|| d\tau, \\ ||\phi_{3,n}(t)|| &\leq \frac{\vartheta^{1-\alpha}}{\Gamma(\alpha)} f_3 \int_0^t ||\phi_{3,n-1}(\tau)|| d\tau, \\ ||\phi_{4,n}(t)|| &\leq \frac{\vartheta^{1-\alpha}}{\Gamma(\alpha)} f_4 \int_0^t ||\phi_{4,n-1}(\tau)|| d\tau. \end{aligned} \tag{9}$$

Thus,

$$\mathcal{S}_n(t) = \sum_{i=1}^{n} \phi_{1,i}(t), \qquad \mathcal{C}_n(t) = \sum_{i=1}^{n} \phi_{2,i}(t),$$
$$\mathcal{I}_n(t) = \sum_{i=1}^{n} \phi_{3,i}(t), \qquad \mathcal{R}_n(t) = \sum_{i=1}^{n} \phi_{4,i}(t).$$

In the following theorem, the existence of the solution will be proved.

Theorem 7.2. *The solutions of Eq. (1) exist if there exists* t_1 *such that*

$$\frac{\vartheta^{1-\alpha}}{\Gamma(\alpha)} t_1 f_j < 1.$$

Proof. Utilizing the iterative method in conjunction with (8) and (9), we can deduce that

$$||\phi_{1,n}(t)|| \leq ||\mathcal{S}_n(0)||[\frac{\vartheta^{1-\alpha}}{\Gamma(\alpha)} f_1 t]^n, \qquad ||\phi_{2,n}(t)|| \leq ||\mathcal{C}_n(0)||[\frac{\vartheta^{1-\alpha}}{\Gamma(\alpha)} f_2 t]^n,$$
$$||\phi_{3,n}(t)|| \leq ||\mathcal{I}_n(0)||[\frac{\vartheta^{1-\alpha}}{\Gamma(\alpha)} f_3 t]^n, \qquad ||\phi_{4,n}(t)|| \leq ||\mathcal{R}_n(0)||[\frac{\vartheta^{1-\alpha}}{\Gamma(\alpha)} f_4 t]^n.$$

As a result, the system possesses a solution and maintains continuity. Moving forward, we will illustrate that the mentioned functions serve as a solution for the model described in (6). Our assumption is

$$\mathcal{S}(t) - \mathcal{S}(0) = \mathcal{S}_n(t) - \mathcal{B}_{1,n}(t), \qquad \mathcal{C}(t) - \mathcal{C}(0) = \mathcal{C}_n(t) - \mathcal{B}_{2,n}(t),$$
$$\mathcal{I}(t) - \mathcal{I}(0) = \mathcal{I}_n(t) - \mathcal{B}_{3,n}(t), \qquad \mathcal{R}(t) - \mathcal{R}(0) = \mathcal{R}_n(t) - \mathcal{B}_{4,n}(t).$$

Therefore,

$$\begin{aligned} ||\mathcal{B}_{1,n}(t)|| &= ||\frac{\vartheta^{1-\alpha}}{\Gamma(\alpha)} \int_0^t (\mathfrak{L}_1(\tau, \mathcal{S}) - \mathfrak{L}_1(\tau, \mathcal{S}_{n-1}))d\tau|| \\ &\leq \frac{\vartheta^{1-\alpha}}{\Gamma(\alpha)} \int_0^t ||\mathfrak{L}_1(\tau, \mathcal{S}) - \mathfrak{L}_1(\tau, \mathcal{S}_{n-1})||d\tau \\ &\leq \frac{\vartheta^{1-\alpha}}{\Gamma(\alpha)} f_1 ||\mathcal{S} - \mathcal{S}_{n-1}||t. \end{aligned}$$

By repeatedly applying the mentioned method, we obtain a result of

$$||\mathcal{B}_{1,n}(t)|| \leq [\frac{\vartheta^{1-\alpha}}{\Gamma(\alpha)}t]^{n+1} f_1^{n+1} k.$$

At $t = t_1$, we get

$$||\mathcal{B}_{1,n}(t)|| \leq [\frac{\vartheta^{1-\alpha}}{\Gamma(\alpha)}t_1]^{n+1} f_1^{n+1} k.$$

Let n approach infinity. Then, it is easy to see that $||\mathcal{B}_{1,n}(t)|| \to 0$. Similarly, we can demonstrate the same result for $||\mathcal{B}_{j,n}(t)||$, $j = 2, 3, 4$. The proof is complete. □

Theorem 7.3. *Equipped with an initial condition, the solution of (1) is unique if*

$$1 - \frac{\vartheta^{1-\alpha}}{\Gamma(\alpha)} f_1 t > 0.$$

Proof. To establish the uniqueness of the solution, let us consider the scenario where the system possesses an additional solution, such as $\mathcal{S}_1(t)$, $\mathcal{C}_1(t)$, $\mathcal{I}_1(t)$, and $\mathcal{R}_1(t)$. Then,

$$\mathcal{S}(t) - \mathcal{S}_1(t) = \frac{\vartheta^{1-\alpha}}{\Gamma(\alpha)} \int_0^t (\mathfrak{L}_1(\tau, \mathcal{S}) - \mathfrak{L}_1(\tau, \mathcal{S}_1)) d\tau.$$

Therefore,

$$||\mathcal{S}(t) - \mathcal{S}_1(t)|| = \frac{\vartheta^{1-\alpha}}{\Gamma(\alpha)} \int_0^t ||\mathfrak{L}_1(\tau, \mathcal{S}) - \mathfrak{L}_1(\tau, \mathcal{S}_1)|| d\tau.$$

From LC (7), it can be deduced that

$$||\mathcal{S}(t) - \mathcal{S}_1(t)|| \leq \frac{\vartheta^{1-\alpha}}{\Gamma(\alpha)} f_1 t ||\mathcal{S}(t) - \mathcal{S}_1(t)||.$$

Thus,

$$||\mathcal{S}(t) - \mathcal{S}_1(t)||(1 - \frac{\vartheta^{1-\alpha}}{\Gamma(\alpha)} f_1 t) \leq 0.$$

Subsequently, $||\mathcal{S}(t) - \mathcal{S}_1(t)|| = 0$, which implies that $\mathcal{S}(t) = \mathcal{S}_1(t)$. Likewise, we can demonstrate the same equality for $\mathcal{C}$, $\mathcal{I}$, and $\mathcal{R}$. □

8 Numerical Method

We will present the approximate solutions for the fractional-order C-19 SCIRS model using the fractional Euler method (FEM) for the CFD. Additionally, we will provide simulations to predict the transmission of C-19 worldwide. To offer a more concise representation, we will express the system described in Eq. (1) as:

$$\vartheta^{\alpha-1}{}^{C}\mathfrak{D}_t^{\alpha} w(t) = y(t, w(t)), \qquad w(0) = w_0,\ 0 \le t \le T < \infty, \tag{10}$$

where $w = (\mathcal{S}, \mathcal{C}, \mathcal{I}, \mathcal{R}) \in \Re_+^4$, the initial vector is $w_0 = (\mathcal{S}_0, \mathcal{C}_0, \mathcal{I}_0, \mathcal{R}_0)$, and the vector function $y(t) \in \Re$ is continuous and satisfies LC

$$||y(w_1(t)) - y(w_2(t))|| \le k||w_1(t) - w_2(t)||, \qquad k > 0.$$

By utilizing a fractional integral operator that corresponds to the CFD on Eq. (10), we obtain a value of

$$w(t) = \vartheta^{1-\alpha}[w_0 + I^{\alpha} y(w(t))], \qquad 0 \le t \le T < \infty.$$

Set $f = \frac{T-0}{N}$ and $t_n = nf$ in which N is natural number and $n = 0, 1, 2, ..., N$. Consider w_n as an approximation of $w(t)$ at $t = t_n$. In [25], the use of the FEM results in obtaining a value of

$$w_{n+1} = \vartheta^{1-\alpha}[w_0 + \frac{f^{\alpha}}{\Gamma(\alpha+1)} \sum_{j=0}^{n} u_{n+1,j} y(t_j, w_j)], \qquad j = 0, 1, 2, ..., N-1,$$

where

$$u_{n+1,j} = (n+1-j)^{\alpha} - (n-j)^{\alpha}, \qquad j = 0, 1, 2, ..., n.$$

The proof of the stability of the acquired method has been demonstrated in Theorem 3.1, as stated in [25].
Therefore, the expression for the solution of system (1) can be written

as:

$$\mathcal{S}_{n+1} = \vartheta^{1-\alpha}[\mathcal{S}_0 + \frac{f^\alpha}{\Gamma(\alpha+1)}\sum_{j=0}^{n} u_{n+1,j} g_1(t_j, w_j)],$$

$$\mathcal{C}_{n+1} = \vartheta^{1-\alpha}[\mathcal{C}_0 + \frac{f^\alpha}{\Gamma(\alpha+1)}\sum_{j=0}^{n} u_{n+1,j} g_2(t_j, w_j)],$$

$$\mathcal{I}_{n+1} = \vartheta^{1-\alpha}[\mathcal{I}_0 + \frac{f^\alpha}{\Gamma(\alpha+1)}\sum_{j=0}^{n} u_{n+1,j} g_3(t_j, w_j)],$$

$$\mathcal{R}_{n+1} = \vartheta^{1-\alpha}[\mathcal{R}_0 + \frac{f^\alpha}{\Gamma(\alpha+1)}\sum_{j=0}^{n} u_{n+1,j} g_4(t_j, w_j)],$$

where $u_{n+1,j} = (n+1-j)^\alpha - (n-j)^\alpha$, $g_1(t, w(t)) = \Lambda - \beta\mathcal{S}(\mathcal{I}+q\mathcal{C}) - \mu\mathcal{S} + \rho\mathcal{R}$, $g_2(t, w(t)) = \beta\mathcal{S}(\mathcal{I}+q\mathcal{C}) - (\eta+\gamma+\mu)\mathcal{C}$, $g_3(t, w(t)) = \eta\mathcal{C} - (\sigma+\mu)\mathcal{I}$ and $g_4(t, w(t)) = \sigma\mathcal{I} + \gamma\mathcal{C} - (\mu+\rho)\mathcal{R}$.

9 Numerical Simulations

In this segment, we provide a computer-generated model that utilizes actual data and employs the MATLAB software for numerical simulation. In order to generate a numerical simulation, it is essential to ascertain the parameter values beforehand. Between June 15th and August 4th, 2022, the global birth rate was 17.688 births per 1000 individuals, while the death rate stood at 7.678 per 1000 individuals. Based on the population on June 15th, denoted as $\mathcal{N}(0) = 7914981120$, we choose values for $\Lambda = 383128.455$ and $\mu = 2.10356 \times 10^{-5}$, and make a decision regarding $\delta = 0.034$ [50]. Furthermore, the initial values on 15 June until 4 August 2022, are as follows: $\mathcal{S}(0) = 7869665900$, $\mathcal{C}(0) = 45000000$, $\mathcal{I}(0) = 15315220$ and $\mathcal{R}(0) = 0$. In this simulation, $\vartheta = 0.99$ and the remaining parameters for C-19 model are acquired via curve fitting.

This simulation covers the entire global population and provides time-scale modeling and simulation for C-19.

Figure 1 illustrates a side-by-side comparison of the non-integer order model (with $\alpha = 0.95$) and the integer order model (with $\alpha = 1$), in addition to actual C-19 case data spanning from June 15 to August 4,

Table 2: Parameter values used in the simulations

Parameters	Value	Reference
Λ	384409.48	Estimated
β	9.08×10^{-11}	Fitted
q	0.1	Fitted
μ	2.10356×10^{-5}	Estimated
ρ	0.02	Fitted
η	0.14	Fitted
γ	0.13	Fitted
σ	0.41	Fitted
δ	0.034	[41]

2022. The obtained results show a relatively good agreement between the predictions of fractional order model and the real data. This highlights the advantages of using fractional order derivative instead of the integer order derivative.

The figures labeled 2-6 display the outcomes of (1) for various values of α. In this specific simulation, the EP corresponds to

$$\mathcal{E}_1 = (7.1606 \times 10^9, 2.1214 \times 10^7, 6.6886 \times 10^6, 2.7472 \times 10^8).$$

Here we give some numerical simulations and show the effect of the suggested control strategy, vaccination, on the prediction of COVID-19. To show the effect of vaccination on the sixth wave in the world, we used the parameters presented in Table 2. To examine how the order of derivation impacts the outcomes of system (1), we conducted calculations for various orders of fractions. The resulting data was then depicted in figures 2-5. The depicted graphs illustrate that the model's results reach a state of equilibrium regardless of the derivative's order. Furthermore, all orders exhibit stability at these EPs. A slight alteration in the derivative's order does not significantly impact the overall behavior of the resulting functions. However, it does generate noticeable differences in the numerical values of the outcomes.

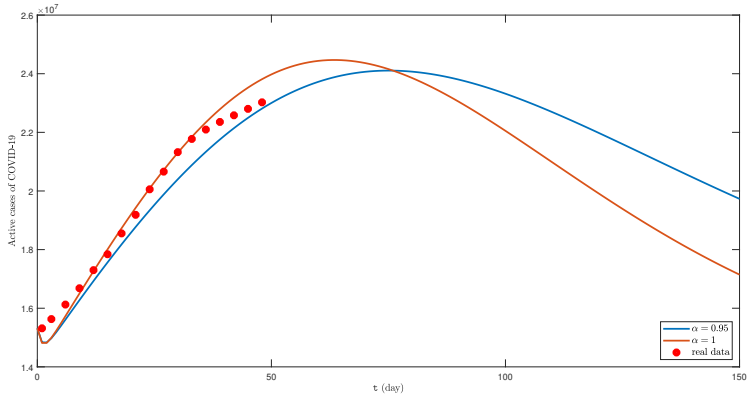

Figure 1: A comparison between the outcomes of the noninteger-order derivative ($\alpha = 0.95$) and the integer-order derivative ($\alpha = 1$) using real data.

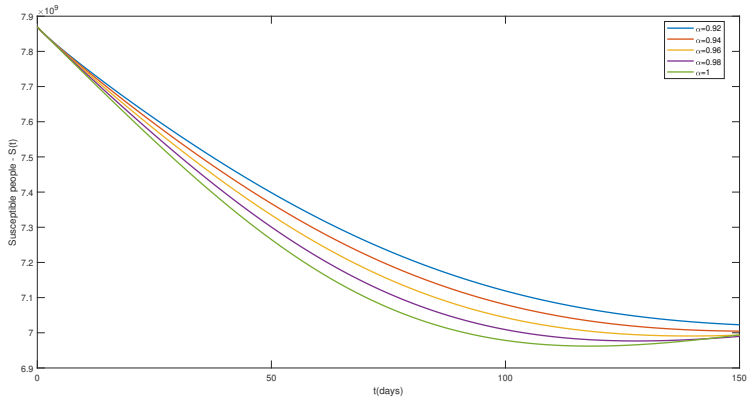

Figure 2: The behavior of $\mathcal{S}(t)$ varies when considering different α values, namely 0.92, 0.94, 0.96, 0.98 and 1.

Table 3: Obtained results of $\mathcal{S}(t), \mathcal{C}(t), \mathcal{I}(t)$ and $\mathcal{R}(t)$ with fractional $\alpha = 0.92$.

t	$\mathcal{S}(t)$	$\mathcal{C}(t)$	$\mathcal{I}(t)$	$\mathcal{R}(t)$
0	7869665900	45000000	15315220	0
1	7843098870	47869061	15016031	23421701
2	7831325094	48801643	15114414	33904354
3	7819931403	49622310	15264752	44069517
⋮	⋮	⋮	⋮	⋮
75	7233054947	75542492	23705548	571413021
76	7227504592	75576453	23723925	576505509
77	7222037702	75602852	23739832	581524789
78	7216654288	75621821	23753305	586470735
⋮	⋮	⋮	⋮	⋮
147	7024813565	66581173	21158777	764731504
148	7024107505	66392860	21099923	765373815
149	7023442889	66204817	21041097	765976031
150	7022818970	66017091	20982314	766538832

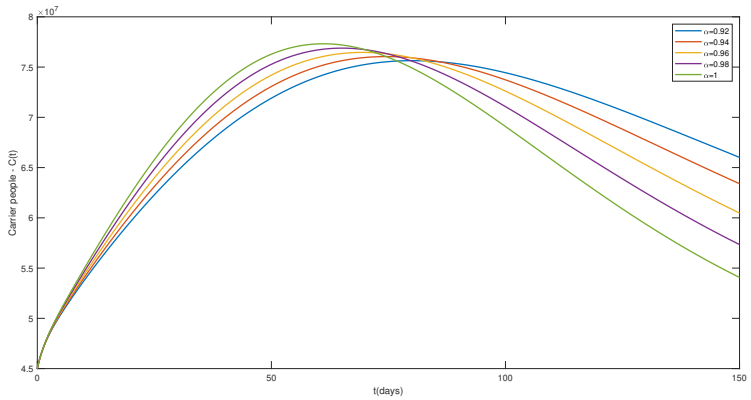

Figure 3: The behavior of $\mathcal{C}(t)$ varies when considering different α values, namely 0.92, 0.94, 0.96, 0.98 and 1.

Table 4: Obtained results of $\mathcal{S}(t), \mathcal{C}(t), \mathcal{I}(t)$ and $\mathcal{R}(t)$ with fractional $\alpha = 0.94$.

t	$\mathcal{S}(t)$	$\mathcal{C}(t)$	$\mathcal{I}(t)$	$\mathcal{R}(t)$
0	7869665900	45000000	15315220	0
1	7842926286	47893075	15010425	23572273
2	7830767861	48855675	15112342	34397717
3	7818923382	49705849	15270651	44966116
⋮	⋮	⋮	⋮	⋮
75	7193184098	76043909	23917420	607963404
76	7187489972	76035397	23922815	613210676
77	7181895651	76018469	23925431	618369791
78	7176401094	75993305	23925322	623440628
⋮	⋮	⋮	⋮	⋮
147	7005181657	64029730	20372738.	782830670
148	7004978254	63818093	20305750	782983739
149	7004816487	63607418	20239014	783095881
150	7004695424	63397746	20172544	783167960

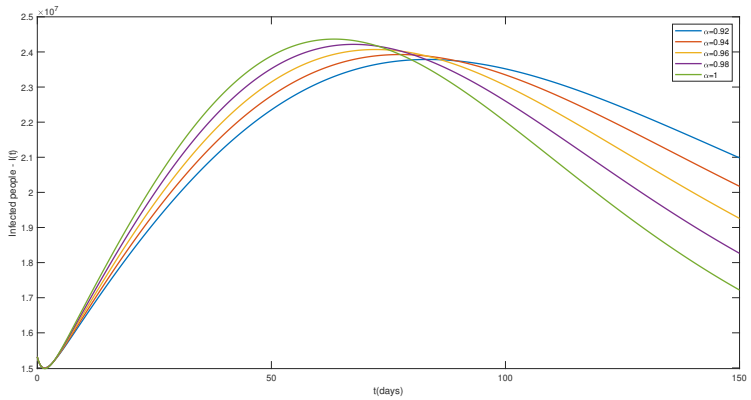

Figure 4: The behavior of $\mathcal{I}(t)$ varies when considering different α values, namely 0.92, 0.94, 0.96, 0.98 and 1.

Table 5: Obtained results of $\mathcal{S}(t), \mathcal{C}(t), \mathcal{I}(t)$ and $\mathcal{R}(t)$ with fractional $\alpha = 0.96$.

t	$\mathcal{S}(t)$	$\mathcal{C}(t)$	$\mathcal{I}(t)$	$\mathcal{R}(t)$
0	7869665900	45000000	15315220	0
1	7842759597	47916816	15004637	23717533
2	7830212838	48909835	15110045	34889027
3	7817908522	49789988	15276568	45868810
⋮	⋮	⋮	⋮	⋮
75	7152684875	76306408	24056385	645234152
76	7146922124	76246650	24045846	650569994
77	7141278282	76177711	24032240	655799957
78	7135753189	76099829	24015641	660923977
⋮	⋮	⋮	⋮	⋮
147	6992251779	61161341	19476157	794446596
148	6992614781	60932412	19402933	794040396
149	6993017466	60705221	19330216	793594461
150	6993458705	60479801	19258020	793109853

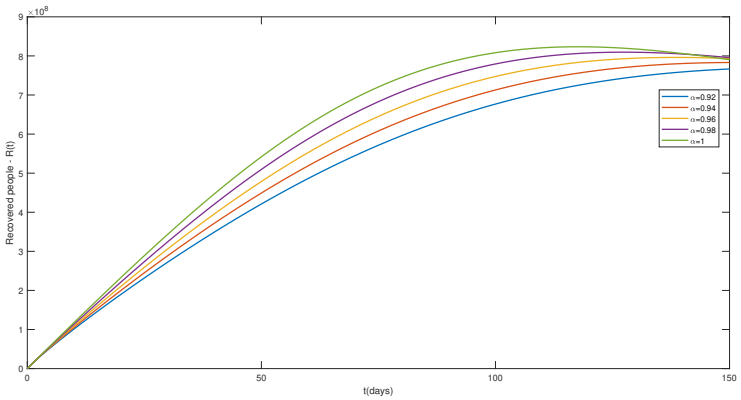

Figure 5: The behavior of $\mathcal{R}(t)$ varies when considering different α values, namely 0.92, 0.94, 0.96, 0.98 and 1.

Table 6: Obtained results of $\mathcal{S}(t), \mathcal{C}(t), \mathcal{I}(t)$ and $\mathcal{R}(t)$ with fractional $\alpha = 0.98$.

t	$\mathcal{S}(t)$	$\mathcal{C}(t)$	$\mathcal{I}(t)$	$\mathcal{R}(t)$
0	7869665900	45000000	15315220	0
1	7842598836	47940281	14998667	23857450
2	7829660209	48964123	15107513	35378116
3	7816887046	49874721	15282496	46777399
⋮	⋮	⋮	⋮	⋮
75	7111930183	76290570	24108958	682896087
76	7106192984	76170643	24079426	688235791
77	7100596700	76040938	24046587	693448898
78	7095140951	75901769	24010537	698535479
⋮	⋮	⋮	⋮	⋮
147	6986719496	58049877	18492486	798810341
148	6987694535	57811089	18415426	797791187
149	6988704664	57574859	18339149	796736039
150	6989748567	57341208	18263663	795646161

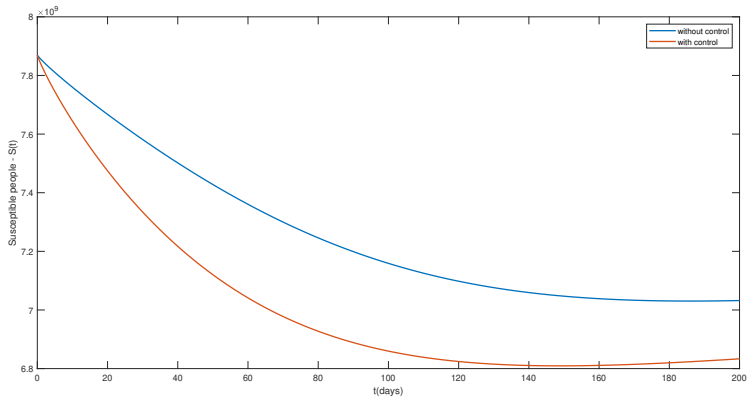

Figure 6: The behavior of $\mathcal{S}(t)$ with $\alpha = 0.9$ in the presence and the absence of control.

Table 7: Obtained results of $\mathcal{S}(t), \mathcal{C}(t), \mathcal{I}(t)$ and $\mathcal{R}(t)$ with fractional $\alpha = 1$.

t	$\mathcal{S}(t)$	$\mathcal{C}(t)$	$\mathcal{I}(t)$	$\mathcal{R}(t)$
0	7869665900	45000000	15315220	0
1	7842444032	47963464	14992517	23991999
2	7829110160	49018539	15104734	35864814
3	7815859180	49960045	15288421	47691678
⋮	⋮	⋮	⋮	⋮
75	7071365014	75957860	24061675	720548543
76	7065768161	75769073	24010108	725786923
77	7060337142	75570180	23955071	730874871
78	7055071222	75361583	23896690	735812709
⋮	⋮	⋮	⋮	⋮
147	6989080458	54780011	17449291	795339215
148	6990689000	54539798	17371169	793676208
149	6992324984	54302961	17294106	791983969
150	6993986925	54069502	17218105	790263943

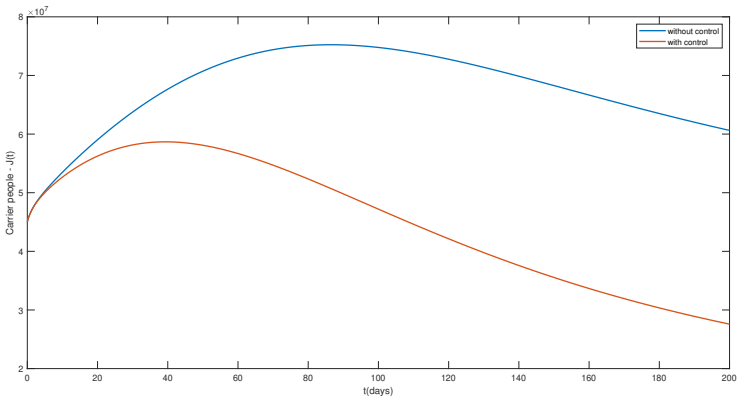

Figure 7: The behavior of $\mathcal{C}(t)$ with $\alpha = 0.9$ in the presence and the absence of control.

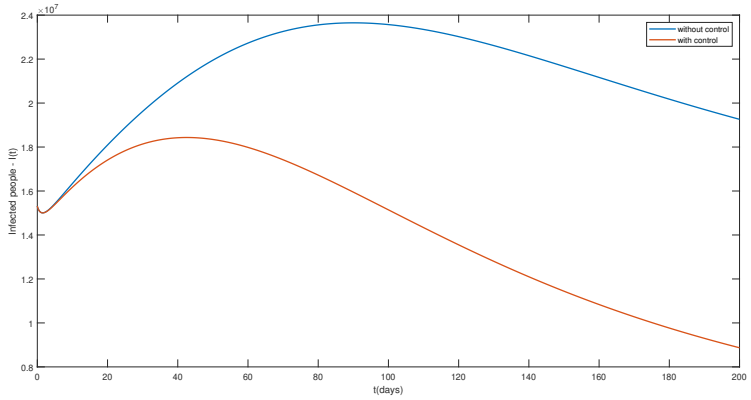

Figure 8: The behavior of $\mathcal{I}(t)$ with $\alpha = 0.9$ in the presence and the absence of control.

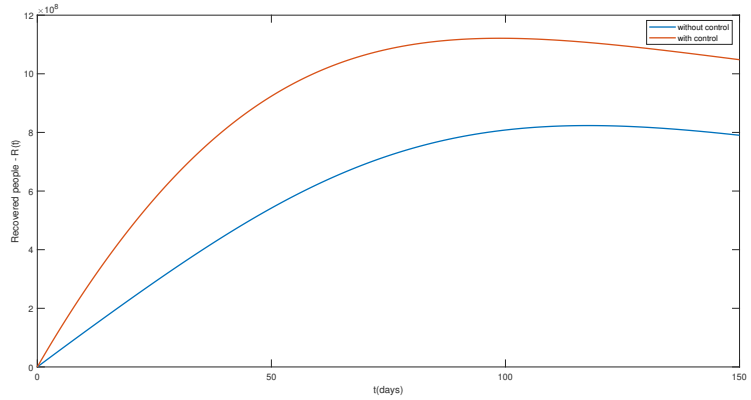

Figure 9: The behavior of $\mathcal{R}(t)$ with $\alpha = 0.9$ in the presence and the absence of control.

10 Conclusions

In this paper, an epidemic SCIRS model for the transmission of Covid-19 in human population with Caputo fractional derivative has been studied. The EPs and the reproduction number have been calculated. We have presented the stability results by applying Lyapunov's second method and LaSalle's invariance principle. The local and global stability of EPs have been presented based on the values of the reproduction number. We proved that, if $\mathcal{R}_0 < 1$, then the EP corresponding to the absence of disease $\mathcal{E}_0$ is locally and globally asymptotically stable and if $\mathcal{R}_0 > 1$, then the positive endemic EP is locally asymptotically stable. The vaccination has been considered as a control strategy and the effect of that has been analyzed. The existence and uniqueness of the solutions of the model have been proven via the fixed point theorem. Additionally, using the fractional Euler method, the approximate solution of the model has been presented. Numerical simulations are utilized, leveraging real data, to forecast the global transmission of C-19. In addition, the real data were used to conduct a comparison between the outcomes of the fractional order system and the integer order system. The findings show that fractional order system shows superior performance in real data management compared to the integer order system. Furthermore, since fractional order derivatives retains the memory of the system, it can serve as a viable substitute for the integer order derivative when modeling natural phenomena.

Acknowledgements
The authors would like to thank anonymous referees for their carefully reading the manuscript and such valuable comments, which has improved the manuscript significantly.

References

[1] S. Abd Alhamid, N. Parisa and N. Jamal, Aerodynamic prediction of time duration to becoming infected with coronavirus in a public place, *Fluids*, **7**(2022), 176.

[2] I. Al-Jahdhami, K. Al-Naamani, A. Al-Mawali and SM. Bennji, Respiratory complications after COVID-19, *Oman Medical Journal*, **37** (2022), e343.

[3] G. Askari, A. Sahebkar, A. Soleimani, D. Mahdavi, A. Rafiee, S. Majeed, M. Khorvash, F. Iraj, B. Elyasi, M. Rouhani and MH. Bagherniya, The efficacy of curcumin-piperine co-supplementation on clinical symptoms, duration, severity, and inflammatory factors in COVID-19 outpatients: a randomized double-blind, placebo-controlled trial, *Trials*, **23**(2022), 1–10.

[4] A. Atangana and S. Qureshi, Mathematical modeling of an autonomous nonlinear dynamical system for malaria transmission using Caputo derivative, *Fractional order analysis: Theory, methods and applications,* (2020), 225–252.

[5] S. M. Aydogan, On a K-dimensional system of hybrid fractional differential equations with multi-point boundary conditions, *Journal of Mathematical Extension*, **15**, (2021), 10.

[6] S. M. Aydogan, D. Baleanu, H. Mohammadi and S. Rezapour, On the mathematical model of Rabies by using the fractional Caputo–Fabrizio derivative, *Advances in Difference Equations*, **2020**, (2020), 382.

[7] S. M. Aydogan, A. Hussain and F. M. Sakar, On a nonlinear fractional-order model of Covid-19 under AB-fractional derivative, *Journal of Mathematical Extension*, **15**, (2021), 11.

[8] W. Badawyeh and M. Abuzaid, Influence of Covid 19 vaccines on diabetes management, *European Journal of Molecular and Clinical Medicine*, **9** (2022), 2682–2693.

[9] D. Baleanu, S. Etemad and S. Rezapour, A hybrid Caputo fractional modeling for thermostat with hybrid boundary value conditions, *Boundary Value Problems*, **2020** (2020), 1–16.

[10] D. Baleanu, B. Ghanbari, J.H. Asad, A. Jajarmi and H.M. Pirouz, Planar system-masses in an equilateral triangle: numerical study

within fractional calculus, *Computer Modeling in Engineering & Sciences*, **124**(3) (2020), 953-968.

[11] D. Baleanu, H. Mohammadi and S. Rezapour, A mathematical theoretical study of a particular system of Caputo–Fabrizio fractional differential equations for the Rubella disease model, *Advances in Difference Equations*, **2020** (2020), 350.

[12] M. Bongiovanni, E. Spada, C. De Angelis, G. Liuzzi and G. Giuliani, SARS-CoV-2 re-infection, vaccination and neutralizing antibodies, *Journal of Infection*, **84** (2022), e120–e121.

[13] N. Brandi, F. Ciccarese, MR. Rimondi, C. Balacchi, C. Modolon, C. Sportoletti, M. Renzulli, F. Coppola and R. Golfieri, An imaging overview of Covid-19 ARDS in ICU patients and its complications: a pictorial review, *Diagnostics*, **12** (2022), 846.

[14] C. Castillo-Chavez and B. Song, Dynamical models of tuberculosis and their applications, *Mathematical Biosciences and Engineering*, **1** (2004), 361–404.

[15] AD. Desai, M. Lavelle, BC. Boursiquot and EY. Wan, Long-term complications of COVID-19, *American Journal of Physiology-Cell Physiology*, **2** (2022), 101012.

[16] K.A. Diethelm, *The Analysis of Fractional Differential Equations*, Springer, **13** (2010).

[17] SA. Elseidy, AK. Awad, M. Vorla, A. Fatima, MA. Elbadawy, D. Mandal and T. Mohamad, Cardiovascular complications in the Post-Acute COVID-19 syndrome (PACS), *IJC Heart and Vasculature*, **40** (2022), 101012.

[18] R. George1, S. M. Aydogan, F. M. Sakar, M. Ghaderi and S. Rezapour, A study on the existence of numerical and analytical solutions for fractional integrodifferential equations in Hilfer type with simulation, *AIMS Mathematics*, **8**, 2023, 5.

[19] R. Hoteit and HM. Yassine, Biological properties of SARS-CoV-2 variants: epidemiological impact and clinical consequences, *Vaccines*, **10** (2022), 919.

[20] R. Kamocki, Pontryagin maximum principle for fractional ordinary optimal control problems, *Mathematical Methods in the Applied Sciences*, **37**(11) (2014), 1668–1686.

[21] A.A. Kilbas, H. M. Srivastava, and J.J. Trujillo, *Theory and Applications of Fractional Differential Equations*, Elsevier, **204** (2006).

[22] SK. Korang, E. von Rohden, AA. Veroniki, G. Ong, O. Ngalamika, F. Siddiqui, S. Juul, EE. Nielsen, JB. Feinberg, JJ. Petersen and C. Legart, Vaccines to prevent Covid-19: a living systematic review with trial sequential analysis and network meta-analysis of randomized clinical trials, *PloS one*, **17** (2022), e0260733.

[23] E. Korompoki, M. Gavriatopoulou, D. Fotiou, I. Ntanasis-Stathopoulos, MA. Dimopoulos and E. Terpos, Late-onset hematological complications post Covid-19: an emerging medical problem for the hematologist, *American Journal of Hematology*, **97** (2022), 119–128.

[24] S. Kreutmair, M. Kauffmann, S. Unger, F. Ingelfinger, NG. Núñez, C. Alberti, D. De Feo, S. Krishnarajah, E. Friebel, C. Ulutekin and S. Babaei, Pre-existing comorbidities shape the immune response associated with severe COVID-19, *Journal of Allergy and Clinical Immunology*, **150** (2022), 312–324.

[25] C. Li and F. Zeng, The finite difference methods for fractional ordinary differential equations, *Numerical Functional Analysis and Optimization*, **34** (2013), 149–179.

[26] J. Losada and J.J. Nieto, Properties of the new fractional derivative without singular kernel, *Prog. Fract. Differ. Appl,* **1(2)**, (2015) 87—92.

[27] KJ. Marks, M. Whitaker, O. Anglin, J. Milucky, K. Patel, H. Pham, SJ. Chai, PD. Kirley, I. Armistead, S. McLafferty and J. Meek, Hospitalizations of children and adolescents with laboratory-confirmed Covid-19—Covid-Net, 14 States, July 2021–January 2022, *Morbidity and Mortality Weekly Report*, **71** (2022), 271.

[28] B. Mohammadaliee, V. Roomi and M. E. Samei, SEIARS model for analyzing COVID-19 pandemic process via ψ-Caputo fractional derivative and numerical simulation, *Scientific Reports*, (2024) 14:723.

[29] J. Myoung, Two years of Covid-19 pandemic: where are we now?, *Journal of Microbiology*, **60** (2022), 235–237.

[30] PA. Naik, KM. Owolabi, M. Yavuz and J. Zu, Chaotic dynamics of a fractional order HIV-1 model involving AIDS-related cancer cells, *Chaos, Solitons and Fractals*, **140** (2020), 110272.

[31] BD. Nuertey, J. Addai, P. Kyei-Bafour, KA. Bimpong, V. Adongo, L. Boateng, K. Mumuni, KM. Dam, EA. Udofia, NA. Seneadza and BN. Calys-Tagoe, Home-based remedies to prevent Covid-19-associated risk of infection, admission, severe disease, and death: a nested case-control study, *Evidence-Based Complementary and Alternative Medicine*, **2022** (2022).

[32] AS. Oke, OI. Bada, G. Rasaq and V. Adodo, Mathematical analysis of the dynamics of COVID-19 in Africa under the influence of asymptomatic cases and re-infection, *Mathematical Methods in the Applied Sciences*, **45** (2022), 137–149.

[33] E. Okyere, FT. Oduro, SK. Amponsah, IK. Dontwi and NK. Frempong, Fractional order malaria model with temporary immunity, *arXiv preprint arXiv:1603.06416*, (2016).

[34] M. Penzes, M. Fekete, A. Feher, A. Lehoczki, T. Csipo and V.I.N.C.E. Fazekas-Pongor, Comorbidities and increased mortality of Covid-19 among the elderly: a systematic review, *Physiol Int.*, (2022) May 16. doi: 10.1556/2060.2022.00206. Epub ahead of print. PMID: 35575986.

[35] C.M.A. Pinto and J.A.T. Machado, Fractional model for malaria transmission under control strategies, *Computers and Mathematics with Applications*, **66** (2013), 908–916.

[36] EB. Postnikov, Estimation of Covid-19 dynamics "on a back-of-envelope": does the simplest SIR model provide quantitative

parameters and predictions?, *Chaos, Solitons and Fractals*, **135** (2020), 109841.

[37] D.R. Powell, J. Fair, R.J. LeClaire, L.M. Moore and D. Thompson, Sensitivity analysis of an infectious disease model, *Proceedings of the International System Dynamics Conference*, (2005).

[38] S. Rajan, M. McKee, C. Hernández-Quevedo, M. Karanikolos, E. Richardson, E. Webb and J. Cylus, What have European countries done to prevent the spread of Covid-19? Lessons from the Covid-19 health system response monitor, *Health Policy*, **126** (2022), 355–361.

[39] S. Rezapour, H. Mohammadi and M. E. Samei, SEIR epidemic model for Covid-19 transmission by Caputo derivative of fractional order, *Advances in difference equations*, **2020** (2020), 1–19.

[40] S. Rezapour, F. M. Sakar, H. Mohammadi and E. Ravash, Some results on a system of multiterm fractional integrodifferential equations, *Turkish Journal of Mathematics*, **44**, (2020), 6.

[41] PJ. Richardson, BW. Robinson, DP. Smith and J. Stebbing, The AI-assisted identification and clinical efficacy of baricitinib in the treatment of Covid-19, *Vaccines*, **10** (2022), 951.

[42] M. E. Samei, H. Zanganeh and S. M. Aydogan, Investigation of a class of the singular fractional integro-differential quantum equations with multi-step methods, *Journal of Mathematical Extension*, **15** (2021).

[43] NR. Sasmita, M. Ikhwan, S. Suyanto and V. Chongsuvivatwong, Optimal control on a mathematical model to pattern the progression of coronavirus disease 2019 (Covid-19) in Indonesia, *Global Health Research and Policy*, **5** (2020), 1–12.

[44] EM. Shaiful and MI. Utoyo, A fractional-order model for HIV dynamics in a two-sex population, *International Journal of Mathematics and Mathematical Sciences*, **2018** (2018), Article ID 6801475.

[45] P. Sookaromdee and V. Wiwanitkit, Comment on "re-infection with SARS-CoV-2 in solid-organ transplant recipients", *Transplant Infectious Disease*, **24** (2022), 3.

[46] NH. Tuan, H. Mohammadi and S. Rezapour, A mathematical model for Covid-19 transmission by using the Caputo fractional derivative, *Chaos, Solitons and Fractals*, **140**, (2020).

[47] P. Van den Driessche and J. Watmough, Reproduction numbers and sub-threshold endemic equilibria for compartmental models of disease transmission, *Mathematical biosciences*, **180** (2002), 29–48.

[48] F. Yoshihara, H. Ohtsu, M. Nakai, S. Tsuzuki, K. Hayakawa, M. Terada, N. Matsunaga, S. Yasuda, H. Ogawa and N. Ohmagari, Renin-angiotensin system blocker and the Covid-19 aggravation in patients with hypertension, diabetes, renal failure, Cerebrocardiovascular disease, or pulmonary disease: report by the Covid-19 registry Japan, *Journal of Cardiology*, **80** (2022), 292–297.

[49] M. Zakerkish, MS. Fooladi, HB. Shahbazian , F. Ahmadi, SP. Payami and M. Dargahi-Malamir, Assessment of mortality rate, need for ICU admission and ventilation in Covid-19 patients with diabetes mellitus, *Qatar Medical Journal*, **1** (2022), 9.

[50] *Worldometer: Covid-19 coronavirus pandemic. American Library Association*. https://www.worldometers.info/coronavirus

Fatemeh Janatolmakan
PhD of Mathematics
Department of Mathematics
Azarbaijan Shahid Madani University
Tabriz, Iran
E-mail: fjanat135@yahoo.com

Vahid Roomi
Associate Professor of Mathematics
Department of Mathematics
Azarbaijan Shahid Madani University
Tabriz, Iran
Insurance Research Center

Tehran, Iran
E-mail: roomi@azaruniv.ac.ir

Tohid Kasbi Gharahasanlou
Assistant Professor of Mathematics
Department of Mathematics and Statistics
Imam Hossein University
Tehran, Iran
E-mail: t.kasbi@ihu.ac.ir